Numerical modeling of waveguides accounting for translational invariance and rotational symmetry

Fabien Treyssede

Available online at www.sciencedirect.com

ScienceDirect

Procedia Engineering 199 (2017) 1562–1567

Procedia Engineering

www.elsevier.com/locate/procedia

X International Conference on Structural Dynamics, EURODYN 2017

Numerical modeling of waveguides accounting for translational invariance and rotational symmetry

Fabien Treyssède[a,*]

[a]*IFSTTAR, GERS, GeoEND, F-44344, Bouguenais, France*

Abstract

The analysis of high-frequency wave propagation in arbitrarily shaped waveguides requires specific numerical methods. A widely spread technique is the so-called semi-analytical finite element (SAFE) formulation. This formulation enables to account for the translational invariance of waveguide problems and leads to a two-dimensional modal problem reduced on the cross-section. Despite this, solving the problem can still be computationally demanding. In order to further reduce the size of the modal problem, this paper presents a SAFE method for waveguides of rotationally symmetric cross-sections. Such structures are encountered in many applications. Typical examples are bars of circular cross-section, regular polygons, and multiwire cables. Numerical results show that the computational effort required for solving the SAFE modal problem is tremendously reduced by accounting for rotational symmetry.

Peer-review under responsibility of the organizing committee of EURODYN 2017.

Keywords: waveguide ; finite element ; rotational symmetry ; modes ; bar ; cable

1. Introduction

Elastic guided waves are of great interest for the inspection of elongated structures. Guided waves are yet multimodal and dispersive, which complicates the physical interpretation of measurement. In practice, modeling tools are required to optimize inspection systems. The modeling of canonical geometries (plates, cylinders) can be done thanks to analytical methods (see *e.g.* [1]).

The analysis of arbitrarily shaped waveguides yet requires numerical methods. A widely spread technique is the so-called semi-analytical finite element (SAFE) formulation [2,3]. It consists in accounting for translational invariance by applying a Fourier transform in the axial direction before finite element discretization. This leads to a two-dimensional modal problem reduced on the cross-section. Despite this, solving the problem can still be computationally demanding when the FE mesh has to be refined and/or the modal density increases (e.g. at high frequency) [4,5]. It is hence desirable to further reduce the size of the modal problem.

This paper presents a SAFE method for rotational symmetric cross-sections, often encountered in practical applications (regular polygons for instance). With a modal approach, accounting for rotational symmetry has indeed two

* Corresponding author. Tel.: +33-240-845-932 ; fax: +33-240-845-997.
E-mail address: fabien.treyssede@ifsttar.fr

1877-7058
Peer-review under responsibility of the organizing committee of EURODYN 2017.
10.1016/j.proeng.2017.09.462

computational benefits: the reduction of the problem size in terms of degrees of freedom and the reduction of the number of modes to compute.

Of particular interest in this work is the modeling of cables in view of nondestructive evaluation. Cables are usually made of individual helical wires, which are coupled through contact conditions. The proper SAFE formulation must be written in a nontrivial helical coordinate system allowing translational invariance along the axis [6]. Such structures yield large size problems involving mesh refinements in the contact regions [5].

Section 2 briefly recalls the SAFE method. The rotational symmetric formulation is presented in Sec. 3. Section 4 is devoted to numerical results. The first test case will be a cylindrical waveguide to validate the approach. Then, a seven-wire strand will be considered. Seven-wire strands are constituted by one central cylindrical wire surrounded by six peripheral helical wires and are widely employed in civil engineering cables.

2. Background: SAFE formulation

The SAFE method is a finite element method dedicated to waveguides. This method aims to account for the translational invariance of the geometry to reduce the size of the problem. The initial full 3D problem is reduced to a 2D modal problem so that one only needs to mesh the cross-section of the waveguide. This section recalls the SAFE formulation. Details can be found in the literature (see *e.g.* [2,3]). Let us denote (x, y) the cross-section coordinates and z the axis coordinate of the waveguide.

First, the strain-displacement relation is written as:

$$\boldsymbol{\epsilon} = (\mathbf{L}_{xy} + \mathbf{L}_z \partial/\partial z)\mathbf{u} \tag{1}$$

where $\mathbf{L}_{xy}$ is the operator containing all terms but derivatives with respect to the z-axis and $\mathbf{L}_z$ is the operator of z-derivatives:

$$\mathbf{L}_{xy} = \begin{bmatrix} \partial/\partial x & 0 & 0 \\ 0 & \partial/\partial y & 0 \\ 0 & 0 & 0 \\ \partial/\partial y & \partial/\partial x & 0 \\ 0 & 0 & \partial/\partial x \\ 0 & 0 & \partial/\partial y \end{bmatrix}, \quad \mathbf{L}_z = \begin{bmatrix} 0 & 0 & 0 \\ 0 & 0 & 0 \\ 0 & 0 & 1 \\ 0 & 0 & 0 \\ 1 & 0 & 0 \\ 0 & 1 & 0 \end{bmatrix}. \tag{2}$$

Then, the SAFE approach consists in applying a time Fourier transform as well as a spatial Fourier transform along z before discretizing the cross-section (x, y) by a finite element method. Inside one finite element e, the displacement field can thus be expressed as follows:

$$\mathbf{u}(x, y, z, t) = \mathbf{N}^e(x, y)\mathbf{U}^e e^{i(kz-\omega t)} \tag{3}$$

where $\mathbf{U}^e$ is the nodal displacement vector and $\mathbf{N}^e$ is the matrix of nodal interpolating functions of the element e. k is the axial wavenumber and ω is the angular frequency.

The variational formulation of three-dimensional elastodynamics yields, from Eqs. (1)–(3), the following matrix equation:

$$\{\mathbf{K}_1 - \omega^2\mathbf{M} + ik(\mathbf{K}_2 - \mathbf{K}_2^{\mathrm{T}}) + k^2\mathbf{K}_3\}\mathbf{U} = \mathbf{F} \tag{4}$$

with the elementary matrices:

$$\begin{aligned} \mathbf{K}_1^e &= \int_{S^e} \mathbf{N}^{e\mathrm{T}}\mathbf{L}_{xy}^{\mathrm{T}}\mathbf{C}\mathbf{L}_{xy}\mathbf{N}^e \mathrm{d}S, \quad \mathbf{K}_2^e = \int_{S^e} \mathbf{N}^{e\mathrm{T}}\mathbf{L}_{xy}^{\mathrm{T}}\mathbf{C}\mathbf{L}_z\mathbf{N}^e \mathrm{d}S, \\ \mathbf{K}_3^e &= \int_{S^e} \mathbf{N}^{e\mathrm{T}}\mathbf{L}_z^{\mathrm{T}}\mathbf{C}\mathbf{L}_z\mathbf{N}^e \mathrm{d}S, \quad \mathbf{M}^e = \int_{S^e} \rho\mathbf{N}^{e\mathrm{T}}\mathbf{N}^e \mathrm{d}S \end{aligned} \tag{5}$$

where $\mathrm{d}S = \mathrm{d}x\mathrm{d}y$ and $\mathbf{C}$ is the matrix of material properties. Setting $\mathbf{F} = \mathbf{0}$ (no acoustic source), Eq. (4) is an eigenvalue problem whose eigensolutions are the guided modes propagating in the translationally invariant structure.

To enforce rotational symmetry, periodic boundary conditions will be needed both on $\mathbf{U}$ and $\mathbf{F}$ as explained in the next section.

3. Accounting for rotational symmetry

The displacement and force vectors are partitioned as follows: $\mathbf{U} = [\mathbf{U}_l^{\mathrm{T}}\ \mathbf{U}_i^{\mathrm{T}}\ \mathbf{U}_r^{\mathrm{T}}]^{\mathrm{T}}$, $\mathbf{F} = [\mathbf{F}_l^{\mathrm{T}}\ \mathbf{F}_i^{\mathrm{T}}\ \mathbf{F}_r^{\mathrm{T}}]^{\mathrm{T}}$, where the subscripts l and r stand for the left and right degrees of freedom (dofs), associated with the left and right boundaries of the rotationally periodic cell of the cross-section (see Fig. 1 for an example). The subscript i is left for the remaining dofs (internal dofs). There are no forces acting on internal dofs because acoustic sources are discarded in the purpose of computing eigenmodes ($\mathbf{F}_i = \mathbf{0}$).

In general, the Bloch-Floquet boundary conditions for a given field ϕ and its dual variable ψ are $\phi_r = \lambda\phi_l$ and $\psi_r = -\lambda\psi_l$ [7,8], where $\lambda = \mathrm{e}^{\mathrm{i}\mu}$ ($\mathrm{i}\mu$ is often called the propagation constant). These conditions hold for a periodicity along straight directions. However, the periodicity to be applied in this paper is of rotational type and concerns a nonscalar field (the displacement vector). The Bloch-Floquet conditions must then be expressed along the circumferential direction in an appropriate frame, namely the cylindrical coordinate system.

Since the displacement components $\mathbf{U}_l$ and $\mathbf{U}_r$ are initially expressed in the (x, y, z) Cartesian frame, they must be transformed to the (r, θ, z) cylindrical frame. Cartesian and cylindrical coordinates are related by $(x, y) = (\rho\cos\theta, \rho\sin\theta)$ ($\rho = 0$ corresponding to the center of rotational symmetry). Let us denote $\mathbf{Q}_l$ and $\mathbf{Q}_r$ the transformation matrices of $\mathbf{U}_l$ and $\mathbf{U}_r$ from the Cartesian to the cylindrical frames. The rotational periodic conditions for the displacement and force vector fields are then:

$$\mathbf{Q}_r\mathbf{U}_r = \lambda\mathbf{Q}_l\mathbf{U}_l \tag{6a}$$

$$\mathbf{Q}_r\mathbf{F}_r = -\lambda\mathbf{Q}_l\mathbf{F}_l \tag{6b}$$

Note that the transformation matrices are block diagonal and comprise three-by-three sub-matrices (for the three components of the displacement vector at every node). These sub-matrices are rotation matrices and are hence orthogonal. Therefore, the following properties hold: $\mathbf{Q}_{l,r}^{-1} = \mathbf{Q}_{l,r}^{\mathrm{T}}$.

Let us denote N the order of the rotational symmetry of the problem. The structure is divided into N rotationally periodic cells. The wave fields at the right boundary of cell N should be equal to the fields at the left boundary of cell 1. This leads to the equation $\lambda^N = 1$ [9], or equivalently: $\mu = 2n\pi/N$, where $n = 0, 1, ...N-1$. The propagation constant can hence be replaced with a user-defined parameter n varying from 0 to $N-1$.

From Eq. (6a), the displacement dofs are related by:

$$\mathbf{U} = \tilde{\mathbf{R}}\tilde{\mathbf{U}}, \quad \tilde{\mathbf{R}} = \begin{bmatrix} \mathbf{I} & \mathbf{0} \\ \mathbf{0} & \mathbf{I} \\ \lambda\mathbf{Q}_r^{-1}\mathbf{Q}_l & \mathbf{0} \end{bmatrix}, \quad \tilde{\mathbf{U}} = \begin{bmatrix} \mathbf{U}_l \\ \mathbf{U}_i \end{bmatrix}. \tag{7}$$

Using the reduced displacement vector $\tilde{\mathbf{U}}$ defined above, Eq. (4) can be rewritten as:

$$\{\tilde{\mathbf{K}}_1 - \omega^2\tilde{\mathbf{M}} + ik(\tilde{\mathbf{K}}_2 - \tilde{\mathbf{K}}_2') + k^2\tilde{\mathbf{K}}_3\}\tilde{\mathbf{U}} = \tilde{\mathbf{R}}^*\mathbf{F} \tag{8}$$

where $\tilde{\mathbf{K}}_i = \tilde{\mathbf{R}}^*\mathbf{K}_i\tilde{\mathbf{R}}$ ($i = 1, 2, 3$), $\tilde{\mathbf{M}} = \tilde{\mathbf{R}}^*\mathbf{M}\tilde{\mathbf{R}}$, $\tilde{\mathbf{K}}_2' = \tilde{\mathbf{R}}^*\mathbf{K}_2^{\mathrm{T}}\tilde{\mathbf{R}}$ and the superscript $*$ denotes complex transpose. These matrices are dependent on the parameter n through the matrix $\tilde{\mathbf{R}}$, which linearly depends on λ.

Accounting for the orthogonality of $\mathbf{Q}_{l,r}$, the expansion of the right hand side of Eq. (8) leads to:

$$\tilde{\mathbf{R}}^*\mathbf{F} = \begin{bmatrix} \mathbf{F}_l + \lambda^*\mathbf{Q}_l^{-1}\mathbf{Q}_r\mathbf{F}_r \\ \mathbf{0} \end{bmatrix} \tag{9}$$

From Eq. (6b), one has: $\mathbf{F}_l + \lambda^*\mathbf{Q}_l^{-1}\mathbf{Q}_r\mathbf{F}_r = (1 - |\lambda|^2)\mathbf{F}_l$. This expression indeed vanishes because $|\lambda| = |\mathrm{e}^{\mathrm{i}\mu}| = 1$ ($\mu \in \mathbb{R}$), so that $\tilde{\mathbf{R}}^*\mathbf{F} = \mathbf{0}$. Therefore, Eq. (8) is the eigensystem to be solved, which accounts both for the translational invariance along the axis (thanks to the SAFE approach) and for the rotational symmetry of the cross-section (thanks to the application of Bloch-Floquet conditions).

As a side remark, left multiplying by the transpose of $\tilde{\mathbf{R}}$, instead of the complex transpose, does not allow to cancel the right hand side in Eq. (8): the product $\tilde{\mathbf{R}}^{\mathrm{T}}\mathbf{F}$ leads to a factor $(1 - \lambda^2)$, not equal to zero (except if $n = 0$).

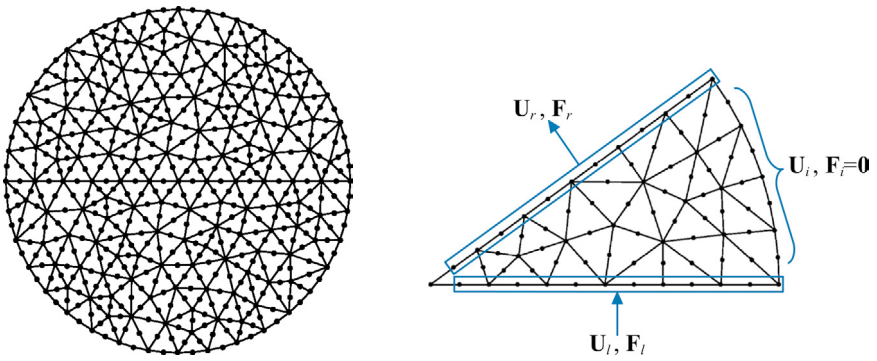

Fig. 1. FE mesh of the cross-section of a cylindrical waveguide. Left: complete model, right: rotationally symmetric cell with $N = 10$.

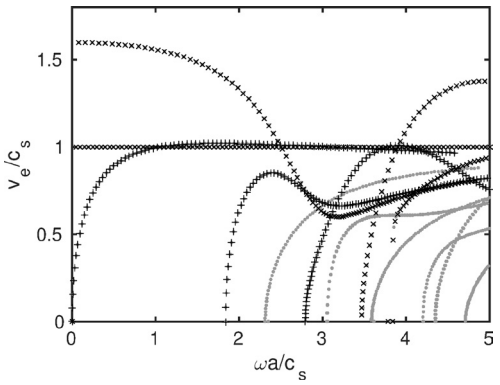

Fig. 2. Energy velocity dispersion curves in a cylindrical waveguide computed with the complete model (grey points), with the reduced model for $n = 0$ (×) and for $n = 1$ (+).

4. Results

Throughout this section, an isotropic material is considered with a Poisson coefficient of 0.3. Dispersion curves will be presented for the dimensionless energy velocity v_e/c_s as function of the dimensionless frequency $\omega a/c_s$, where c_s denotes the shear velocity and a is a characteristic length. The energy velocity v_e can be straightforwardly post-processed from the eigensolutions of the SAFE eigensystems (4) and (8) (see Ref. [6] for instance). The finite element discretization of rotationally periodic cells is generated so that left and right boundaries have a compatible mesh that allows a direct connection between nodes. Six-node triangles are used.

4.1. Cylindrical waveguide

In order to validate the approach, a cylindrical waveguide is considered. The characteristic length a is chosen as the radius of the cylinder.

Owing to the circular cross-section, the angular sector of the elementary cell can be arbitrarily thin. In this example, the rotationally symmetric SAFE model is reduced to a sector of angle $2\pi/10$ (see Fig. 1).

Results are compared with the full SAFE model of a complete circular cross-section, i.e. without accounting for rotational symmetry. Figure 2 plots the dimensionless energy velocity dispersion curves for $n = 0$ and $n = 1$. For $n = 0$, the rotationally symmetric SAFE model gives axisymmetric propagation modes (compressional and torsional modes). The remaining modes, of flexural type, are not axisymmetric and can be obtained for $n = 1, 2, ..., 9$ (in Fig. 2, only $n = 1$ modes are shown for conciseness). Modes computed with both models are in very good agreement.

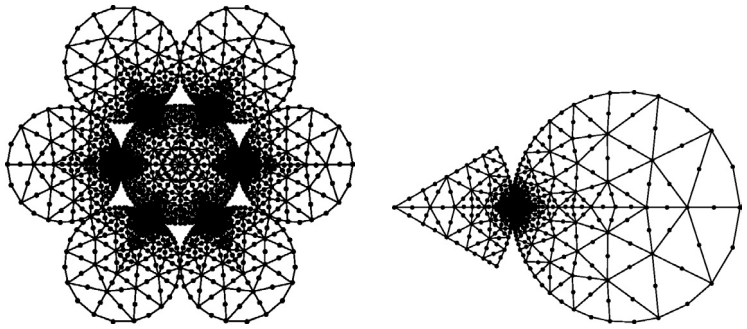

Fig. 3. FE mesh of the cross-section of a seven-wire strand. Left: complete model, right: rotationally symmetric cell ($N = 6$).

Compared to the full SAFE mode, the computational time is reduced by a factor 16 for a given n. Note that in addition to the reduction of the number of dofs (by a factor 10 here), the number of modes to compute for each value of n is reduced to about 5 compared to 25 with the full model, which also contributes to reducing the computational effort.

4.2. Seven-wire strand

A seven-wire strand is now considered. The characteristic length a is chosen as the radius of the central wire. The strand is prestressed with a 0.6% elongation. Because peripheral wires are not straight but helical, the analysis of guided waves requires a specific curvilinear coordinate system, called twisting coordinate system. A twisting system is a particular case of helical system, with zero curvature and a torsion $\tau = 2\pi/L$ (with L denoting the helix pitch of peripheral wires). In this twisting system, the cross-section of the whole structure remains translationally invariant so that guided waves truly exist [6]. The operators of prestressed elastodynamics must be rewritten in the twisting coordinate system yielding expressions for $\mathbf{L}_{xy}$ and $\mathbf{L}_z$ that depend on τ and are different from Eq. (1). The reader may refer to [5,6] for the expressions of these operators and further details about the SAFE modeling of prestressed seven-wire strands. Anyway, the SAFE approach leads to an eigensystem which keeps the same form as Eq. (4).

Now, the number of peripheral wires of the strand yields a rotational symmetry of order 6, which can be further exploited thanks to the procedure described in Sec. 3. Figure 3 shows the complete and reduced FE meshes of the cross-section, refined near interwire regions in order to accurately account for contact phenomena [5]. Note that no contact occurs between peripheral wires so that periodic conditions are only applied to the central wire.

Figure 4 plots the dimensionless energy velocity dispersion curves obtained with the full model and the rotationally symmetric model for $n = 0$ and $n = 1$. Results coincide with each other (the modes calculated for $n = 2, ..., 5$ are not shown for conciseness).

The rotational symmetric model allows reducing the number of dofs by a factor 6 as well as the number of computed modes to about 8 (compared to 40 with the full model). For a given n, this leads to a computational time reduced by a factor 13.

As can be observed in Fig. 4, seven-wire strands are complex structures involving many dispersion curves owing to the coupling between wires. Another advantage of the formulation is the intrinsic classification of modes in terms of their symmetry order n. This can greatly helps the analysis of the dynamic behavior of such complex structures and the interpetation of results.

5. Conclusion

In this paper, a SAFE method has been presented to account for the rotational symmetry of structural waveguides. The method has been tested for cylinders and seven-wire strands. The approach enables to significantly reduce the problem size in terms of degrees of freedom as well as the number of modes to compute. The rotationally symmetric SAFE formulation opens new possibilities for the numerical analysis of complex waveguides in high-frequency

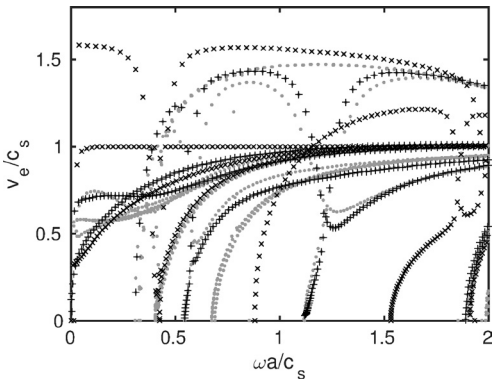

Fig. 4. Energy velocity dispersion curves in a seven-wire strand. Same legend as in Fig. 2.

regime. Of particular interest will be the modeling of open waveguides (i.e. unbounded in the transverse directions) and umbilical power cables used in offshore wind turbine applications. The former involve continua of radiation modes, which leads to the computation of many unwanted modes when absorbing conditions are used. The latter have a more complex architecture than seven-wire strands and involve rotational symmetry of high order. The proposed rotationally symmetric SAFE formulation will enable to significantly reduce the computational effort in the analysis of these types of problem.

Acknowledgements

The author wishes to thank Région Pays de la Loire and the West Atlantic Marine Energy Center for their financial support.

References

[1] B. N. Pavlakovic, M. J. S. Lowe, D. N. Alleyne, P. Cawley, Disperse: A general purpose program for creating dispersion curves, in: Review of Progress in Quantitative NDE, volume 16, 1997, pp. 185–192.
[2] T. Hayashi, W.-J. Song, J. L. Rose, Guided wave dispersion curves for a bar with an arbitrary cross-section, a rod and rail example, Ultrasonics 41 (2003) 175–183.
[3] I. Bartoli, A. Marzani, F. Lanza di Scalea, E. Viola, Modeling wave propagation in damped waveguides of arbitrary cross-section, Journal of Sound and Vibration 295 (2006) 685–707.
[4] F. Treyssède, Spectral element computation of high frequency leaky modes in three-dimensional solid waveguides, Journal of Computational Physics 314 (2016) 341–354.
[5] F. Treyssède, Dispersion curve veering of longitudinal guided waves propagating inside prestressed seven-wire strands, Journal of Sound and Vibration 367 (2016) 56–68.
[6] F. Treyssède, L. Laguerre, Investigation of elastic modes propagating in multi-wire helical waveguides, Journal of Sound and Vibration 329 (2010) 1702–1716.
[7] D. J. Mead, A general theory of harmonic wave propagation in linear periodic systems with multiple coupling, Journal of Sound and Vibration 27 (1973) 235–260.
[8] R. S. Langley, A variational principle for periodic structures, Journal of Sound and Vibration 135 (1989) 135–142.
[9] M. Petyt, Introduction to Finite Element Vibration Analysis, Cambridge University Press, 1990.